Cross-Modal Discrete Representation Learning

Alexander H. Liu SouYoung Jin Cheng-I Jeff Lai Andrew Rouditchenko
Aude Oliva James Glass
Computer Science and Artificial Intelligence Laboratory
Massachusetts Institute of Technology
Cambridge, MA 02139, USA
{alexhliu, souyoung, clai24, roudi, oliva, glass}@mit.edu

Abstract

In contrast to recent advances focusing on high-level representation learning across modalities, in this work we present a self-supervised learning framework that is able to learn a representation that captures finer levels of granularity across different modalities such as concepts or events represented by visual objects or spoken words. Our framework relies on a discretized embedding space created via vector quantization that is shared across different modalities. Beyond the shared embedding space, we propose a Cross-Modal Code Matching objective that forces the representations from different views (modalities) to have a similar distribution over the discrete embedding space such that cross-modal objects/actions localization can be performed without direct supervision. We show that the proposed discretized multi-modal fine-grained representation (e.g., pixel/word/frame) can complement high-level summary representations (e.g., video/sentence/waveform) for improved performance on cross-modal retrieval tasks. We also observe that the discretized representation uses individual clusters to represent the same semantic concept across modalities.

1 Introduction

Toddlers acquire much of their knowledge through grounded learning – visual concepts can be acquired through language, and language acquisition emerges through visual interaction. Inspired by this type of grounded learning, a rich body of representation learning research (Harwath et al., 2018; Miech et al., 2020; Alayrac et al., 2020; Monfort et al., 2021; Luo et al., 2021) has been exploring the potential to learn from multi-modal data such as video-text, video-audio, and image-audio pairs. These works typically focus on learning a joint embedding space between different modalities, in which high-level summary representations are extracted as embedding vectors. These embedding vectors often represent entire video clips, spoken utterances, or sentences as single vectors, and can be useful on tasks such as cross-modal data retrieval, e.g., finding the most similar visual scene according to a spoken language description. The predominant approach to learning these embedding vectors is to use modality-independent encoders, and while this has been successful for downstream retrieval tasks, it makes it difficult to compare the activations of the encoders from different modalities. Further, the space of continuous embedding vectors is unbounded, which makes interpreting the learned representations challenging.

To this end, we propose to jointly learn high-level embedding vector representations with a fine-grained discrete embedding space that is shared across different modalities. The discrete embedding space enables model interpretability since there are a finite number of embedding vectors which are shared across modalities. Besides the shared embedding space, we propose a Cross-Modal Code Matching (CMCM) objective that guides the embedding space to capture cross-modal correspondences of concepts, actions, and words. This not only improves downstream performance on retrieval, but also allows us to better interpret what the model recognized through cross-modal grounded learning.

To verify the effectiveness of our proposed learning framework, we conducted experiments in several cross-modal domains, including video-text, video-audio, and image-audio. We found consistent improvements over baseline models, verifying that the gain was not restricted to the particular choice of network architecture, input modalities, or dataset. We also demonstrate the interpretability of the fine-grained discrete representations by showing the cross-modal relations between the embedding vectors and semantic concepts appearing in the input modalities. Our approach also enables cross-modal concept localization without requiring any labels during training.

Proceedings of the 60th Annual Meeting of the Association for Computational Linguistics
Volume 1: Long Papers, pages 3013 - 3035

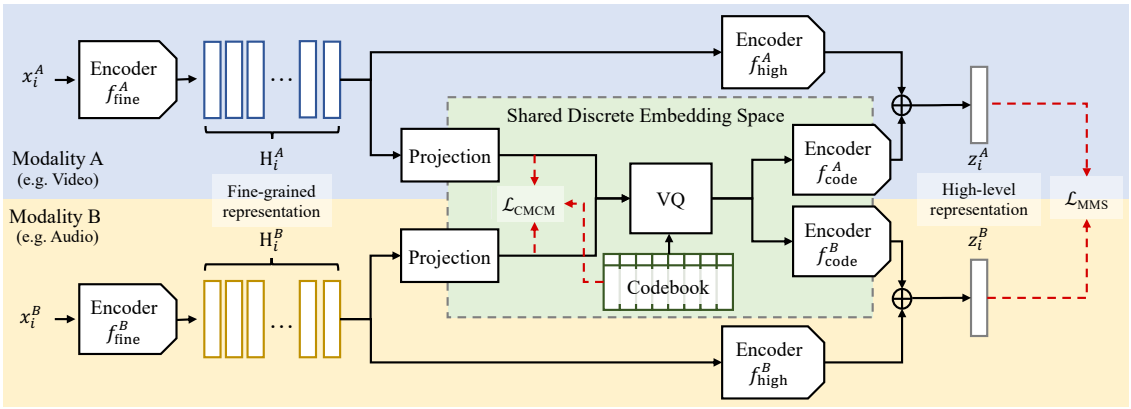

Figure 1: An overview of the proposed framework. The proposed shared discrete embedding space (green region, described in Section 2.2) is based on a cross-modal representation learning paradigm (blue/yellow regions, described in Section 2.1). The proposed Cross-Modal Code Matching $\mathcal{L}_{\text{CMCM}}$ objective is detailed in Section 2.3 and Figure 2.

2 Methodology

Figure 1 provides an overview of the proposed framework. We begin by describing the two-branch cross-modal representation learning paradigm in Section 2.1 (the blue and yellow regions). Next, we introduce our shared discrete embedding space in Section 2.2 (the green region). Finally, in Section 2.3 and Figure 2, we introduce the Cross-Modal Code Matching objective which guides the model to learn semantically meaningful representations through the shared discrete embedding space.

2.1 Cross-Modal Learning Paradigm

Given a set of data $\mathcal{X} = \{(x_i^A, x_i^B)\}_{i=1}^N$ of size N where each instance x_i is instantiated in different modalities A and B (e.g. video and its corresponding caption), the goal is to derive high-level representative vectors (z_i^A, z_i^B) for each instance (x_i^A, x_i^B) that capture the cross-modal relation measured by a choice of similarity function $S(\cdot, \cdot)$.

For a specific modality $M \in \{A, B\}$, a common first step is to encode raw data x_i^M into a sequence of "fine-grained" latent features H_i^M with a modality-specific neural network f_{fine}^M, i.e. $H_i^M = f_{\text{fine}}^M(x_i^M)$. The fine-grained representations H_i^M can express different kinds of raw data, such as video, audio, or sentences, as a sequence of vectors $\{h_{i,1}^M, ..., h_{i,L}^M\}$ of length L. In the second step, a "high-level" representation z_i^M can be derived by summarizing the fine-grained latent features H_i^M with another encoding function f_{high}^M that reduces the sequence into a single vector, i.e. $z_i^M = f_{\text{high}}^M(H_i^M)$.

For example, with modality A being video, raw data x_i^A can be treated as a sequence along time and space and encoded into fine-grained representations $H_i^A = \{h_{i,l}^A\}_{l=1}^L$ by choosing f_{fine}^A to be a Residual Network (He et al., 2016). For the second step, a natural choice for f_{high}^A to derive the high-level representation z_i^A would be a mean pooling function over the time and spatial axes (arranged along l).

With the sets of high-level representations $\{z_i^A\}_{i=1}^N$ and $\{z_j^B\}_{j=1}^N$ from different modalities, we can measure the cross-modal relation between any pair of representations (z_i^A, z_j^B) with some similarity function[1] $S(\cdot, \cdot)$. The final step in this paradigm is to adopt an objective function that maximizes the similarity score between "positive" pairs (where $i = j$, and thus the true pairs) and minimizes the similarity score between "negative" pairs (where $i \neq j$, and thus imposter pairs).

While different objective functions, such as Semi-Hard Negative Mining (Schroff et al., 2015) (SHN) and Noise Constrastive Estimation (Gutmann and Hyvärinen, 2010) (NCE), have been studied in prior work, we focused on the Masked Margin Softmax (Ilharco et al., 2019) (MMS) loss

$$\mathcal{L}_{\text{MMS}} = -\frac{1}{N}\sum_{i=1}^{N} \log \frac{e^{S(z_i^A, z_i^B) - M}}{e^{S(z_i^A, z_i^B) - M} + \sum_{j=1}^{N} I_{i \neq j} e^{S(z_i^A, z_j^B)}}, \quad (1)$$

where the margin M is a hyperparameter to encourage a higher similarity for positive pairs. The MMS loss $\mathcal{L}_{\text{MMS}}$ can be seen as an application of the InfoNCE (Oord et al., 2018) loss with a margin.

The effectiveness of the described cross-modal learning paradigm has been shown by recent works that achieved state-of-the-art results on benchmark

[1] While we used dot product throughtout this work, we also found euclidean distance works well in practice.

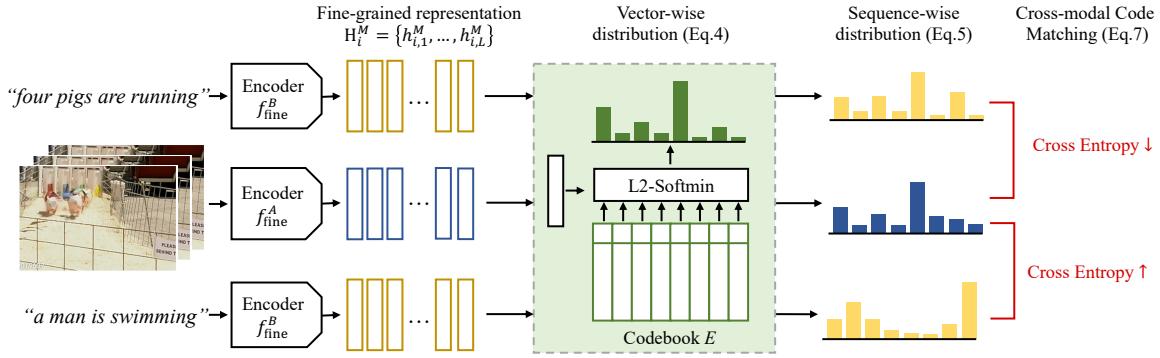

Figure 2: Our proposed Cross-Modal Code Matching objective (described in Section 2.3), which encourages the model to use similar codewords for matching cross-modal pairs.

datasets in different cross-modal scenarios such as video-text (Luo et al., 2021), video-audio (Monfort et al., 2021; Rouditchenko et al., 2020), and image-text (Radford et al., 2021).

2.2 Shared Discrete Embedding Space

While the high-level representations (z_i^A, z_i^B) given by the cross-modal learning paradigm benefit end tasks such as data retrieval, the representations cannot be easily interpreted by humans. To obtain fine-grained representations that are more interpretable, we introduce a Vector Quantization (Oord et al., 2017) (VQ) mechanism after obtaining the H_i^M representations. Formally, with an auxiliary embedding table $E = \{e_1, e_2, ..., e_V\}$ of size V, which we refer to as the *codebook*, vector quantization is performed on each fine-grained representation $h_{i,l}^M \in H_i^M$ of modality $M \in \{A, B\}$ with $\bar{h}_{i,l}^M = f^M(h_{i,l}^M) + \text{sg}(e_v - f^M(h_{i,l}^M))$, where f^M is a modality specific projection network to project the input to the shared embedding space, $v = \arg\min_{k \in V} \|h_{i,l}^M - e_k\|_2$, and $\text{sg}(\cdot)$ is the stop-gradient operator proposed in straight-through gradient estimation (Bengio et al., 2013) that treats the input as constant during backpropagation. In other words, each vector $h_{i,l}^M$ will be replaced by its nearest neighbor e_v, which we refer to as the *codeword*, in the codebook E. The codebook is randomly initialized and updated with the exponential moving average (Oord et al., 2017) given the fine-grained representations (more details in Section A of the Appendix).

We trained the shared embedding space jointly with the rest of the framework by modifying the high-level representations z_i^M to include the discretized fine-grained representations as $z_i^M = f_{\text{high}}^M(H_i^M) + f_{\text{code}}^M(\bar{H}_i^M)$, where f_{code}^M is, similar to f_{high}^M, the encoding function for summarizing the sequence of quantized fine-grained representations (e.g., an average pooling function over l). Having such a discrete embedding space allows humans to better interpret the learned embeddings since they are shared across modalities and there are a finite number of them.

2.3 Cross-Modal Code Matching

Ideally, the codebook should be shared across different modalities since the quantization method is independent to the input modality. However, as we demonstrate in Section F of the Appendix, the model will learn to partition the codebook into modality-specific subspaces due to the significant difference between fine-grained representations from different modalities. To learn a shared embedding space that is invariant to input modality, we propose the Cross-Modal Code Matching objective which encourages the model to focus more on the semantic aspect of the input, as illustrated in Figure 2.

For each vector $h_{i,l}^M$ in the fine-grained representation sequence H_i^M encoded from an instance x_i^M of modality M, we first define the probability of $h_{i,l}^M$ belonging to the codeword e_v as the Softmin function of their Euclidean distance, $P(e_v|h_{i,l}^M) = \frac{\exp(-\|f^M(h_{i,l}^M) - e_v\|_2)}{\sum_{k \in V} \exp(-\|f^M(h_{i,l}^M) - e_k\|_2)}$. Note that this definition assigns higher a probability to codewords that are closer to the fine-grained representation, where the closest codeword is used to perform vector quantization. We can then define the sequence-level probability distribution over the codebook as the average of the fine-grained distribution, $P(e_v|H_i^M) = \frac{1}{L}\sum_l P(e_v|h_{i,l}^M)$, which is the normalized frequency of codeword usage for a given sequence of fine-grained representations. Next, for a pair of cross-modal data (x_i^A, x_j^B), we define their *code similar-*

ity as the negative symmetric cross entropy of probability distribution over the codebook $S_{\text{code}}(x_i^A, x_j^B) = \sum_v P(e_v|H_i^A) \log P(e_v|H_j^B) + \sum_v P(e_v|H_j^B) \log P(e_v|H_i^A)$.

Finally, we define the *Cross-Modal Code Matching (CMCM)* objective using code similarity as

$$\mathcal{L}_{\text{CMCM}} = -\frac{1}{N}\sum_{i=1}^{N} \log \frac{e^{S_{\text{code}}(x_i^A, x_i^B)}}{e^{S_{\text{code}}(x_i^A, x_i^B)} + \sum_{j \neq i} e^{S_{\text{code}}(x_i^A, x_j^B)}}. \quad (2)$$

Intuitively, the proposed objective encourages the model to represent the input (x_i^A, x_j^B) with similar codewords for positive pairs ($i = j$) and non-matching codewords for negative pairs ($i \neq j$). As a consequence, each codeword is expected to be a modality invariant representation of a more fine-grained concept, action, or word that can be discovered from cross-modal data. For example, a codeword could correspond to both the visual scene of a man juggling, and also the spoken word "juggling," as we demonstrate in our experimental results in Table 2 and Figure 4.

The full objective of our proposed cross-modal representation learning framework is the combination of objectives at different levels $\mathcal{L} = \mathcal{L}_{\text{MMS}} + \alpha\mathcal{L}_{\text{CMCM}}$, where α controls the weight between the two terms. Empirically, we found $\alpha = 0.1$ worked well across different settings. Please refer to Section C and D in Appendix for ablation study and comparison to possible alternatives to our method.

3 Related work

Examples of the cross-modal learning paradigm. As described in Section 2.1, many of the existing methods for cross-modal learning fit into the paradigm where encoders are modality-independent. This paradigm has been shown to be effective by achieving state-of-the-art retrieval performance on benchmark datasets with the modality pairs that we considered in this work: video-text (Bain et al., 2021; Luo et al., 2021), video-audio (Monfort et al., 2021; Rouditchenko et al., 2020), and image-audio (Harwath et al., 2018, 2020). While these prior works relied on different pre-training datasets, model architectures, and objective functions, they all leverage modality-independent encoders. One of the most important features of this paradigm is the fixed inference time for retrieval. Since the encoders are modality-independent, embedding vectors for samples in a given modality can be computed without using any samples from the other modality. Thus retrieval only involves computing the dot product between embedding vectors from two different modalities. As a consequence, these models are more flexible for large-scale retrieval, and the embedding vectors from each modality can be used independently for other downstream tasks.

Other cross-modal learning frameworks. In contrast to the aforementioned works, some methods leverage cross-modal relations within the encoders instead of using modality-independent encoders. This has been done with both cross-modal encoders (Lei et al., 2021; Luo et al., 2021) and cross-modal attention mechanisms (Miech et al., 2018; Liu et al., 2019b,a; Gabeur et al., 2020). However, the cross-modal interactions increase the complexity for retrieval since every instance of a specific modality must be used as input with every instance of another modality to obtain the embedding vectors. With m and n samples in the modalities respectively, this increases the complexity from the modality-independent approach from $\mathcal{O}(m+n)$ to $\mathcal{O}(mn)$. Further, it also makes analysis of the embedding vectors from any individual modality challenging and inhibits single-modality downstream tasks. Our proposed framework builds on the modality-independent approach to enable light-weight retrieval, but it also enables cross-modal interaction through our proposed codebook and Cross-Modal Code Matching objective.

Uncovering semantic-level correspondences. Image-audio models have been shown to discover spoken words and visual objects without supervision through retrieval tasks (Synnaeve et al., 2014; Harwath and Glass, 2015; Harwath et al., 2017; Kamper et al., 2018), and the audio embedding vectors have been shown to cluster into word-like speech units (Harwath and Glass, 2017; Wang and Hasegawa-Johnson, 2019; Harwath et al., 2020). Some work has studied the ability of video-audio models to relate spoken words to visual objects and actions in videos (Boggust et al., 2019; Rouditchenko et al., 2020). However, none of these models incorporated a shared embedding space that enabled modality-invariant representations. VQ units have been used in the audio encoder of an image-audio model (Harwath et al., 2020), which allowed it to capture the hierarchical structure of spoken language. While our proposed framework is similar in that it also discretizes the audio sequence

Table 1: Cross-Modal retrieval results on S-MiT, Places, and MSR-VTT.

Modality *A*-*B* / Dataset Method	Visual Retrieval ($B \rightarrow A$)				Language Retrieval ($A \rightarrow B$)			
	R@1 ↑	R@5 ↑	R@10 ↑	MnR ↓	R@1 ↑	R@5 ↑	R@10 ↑	MnR ↓
Video-Audio / S-MiT (Monfort et al., 2021)								
S-MiT (Monfort et al., 2021)	32.1	58.9	68.6	-	32.3	57.9	68.1	-
Our Baseline†	30.2	57.3	68.5	41.9	29.7	57.2	68.7	28.5
Proposed	**34.3**	**61.3**	**72.0**	**33.5**	**34.0**	**61.6**	**71.7**	**22.5**
Image-Audio / Places (Harwath et al., 2017)								
ResDAVEnet (Harwath et al., 2018)*	30.9	63.6	74.2	20.2	26.4	58.5	71.2	21.6
ResDAVEnet-VQ (Harwath et al., 2020)*	34.9	70.2	79.4	15.0	32.7	65.6	77.0	18.0
Our Baseline†	43.8	74.1	82.4	15.8	40.4	73.3	82.5	10.9
Proposed	**46.5**	**77.4**	**85.8**	**13.7**	**45.4**	**77.7**	**85.9**	**8.9**
Video-Text / MSR-VTT (Xu et al., 2016)								
Frozen-in-Time (Bain et al., 2021)	31.0	59.5	70.5	-	-	-	-	-
CLIP4Clip-meanP (Luo et al., 2021)	43.1	70.4	80.8	16.2	-	-	-	-
CLIP4Clip-tightT (Luo et al., 2021)	40.2	71.5	80.5	**13.4**	-	-	-	-
Our Baseline†	42.6	71.2	80.8	15.5	**43.0**	70.9	80.9	12.5
Proposed	**43.4**	**72.3**	**81.2**	14.8	42.5	**71.2**	**81.1**	**12.0**

† Existing model reproduced with $\mathcal{L}_{\text{MMS}}$ for fair comparison, see Table 3 in the Appendix for more detail.
* Results obtained by running the official code and pre-trained models, see Appendix for more details.

with VQ units, our work differs significantly by capturing the cross-modal interactions between visual and audio inputs in the shared embedding space rather than solely capturing the tree structure of speech. Further, besides image-audio data, our proposed framework can handle video-audio and video-text data.

4 Experiments

4.1 Setup

To demonstrate the generalizability of the proposed method, we tested our framework on different cross-modal datasets and baseline models that fit into the cross-modal learning paradigm. All setups are listed below and summarized in Table 3 of the Appendix. For training the proposed model, we randomly initialized all the modules related to the discrete shared embedding space and trained them jointly with the rest of the framework (see Figure 1). Unless otherwise specified, (1) we "warm-started" our proposed framework by initializing it with the modality-specific encoders (namely, f^M_{fine} and f^M_{high}) from the baseline models; (2) both the projection network f^M and the encoder network f^M_{code} are single linear layers; (3) the codebook size is set to 1024. Please refer to Section B in the Appendix for more implementation details.

Video-Audio: S-MiT (Monfort et al., 2021) contains over 500k pairs of 3-second video and corresponding spoken audio captions averaging 8 seconds. We followed the official protocol to train on the training set of 500k pairs, use the validation set of 10k pairs for development and analysis, and report the retrieval result on a 1k search space over 5 runs randomly sampled from a held-out test set. We selected the same baseline model used on the dataset (Monfort et al., 2021), which contains a visual encoder composed of a ResNet-152 pre-trained on ImageNet (Deng et al., 2009) and TSM ResNet-50 (Lin et al., 2019) pre-trained on M-MiT (Monfort et al., 2019). The audio encoder is a randomly initialized 1D-ResNet (Harwath et al., 2018) designed specifically for spectrograms. The shared embedding space has the dimension of 4096, matching the encoders in the baseline model.

Image-Audio: Places (Harwath et al., 2017) contains over 400k pairs of images from the Places 205 dataset (Zhou et al., 2014) and corresponding spoken audio captions averaging 10 seconds. We followed the previous works (Harwath et al., 2018, 2020) to use the training set of 400k pairs and report results on the validation set of 1k pairs. We select ResDAVEnet (Harwath et al., 2018) as the baseline model where the visual encoder is a ResNet-50 pre-trained on ImageNet (Deng et al., 2009) and the audio encoder is a randomly initialized 1D-ResNet (Harwath et al., 2018) designed specifically for spectrograms. The shared embedding space has the dimension of 1024.

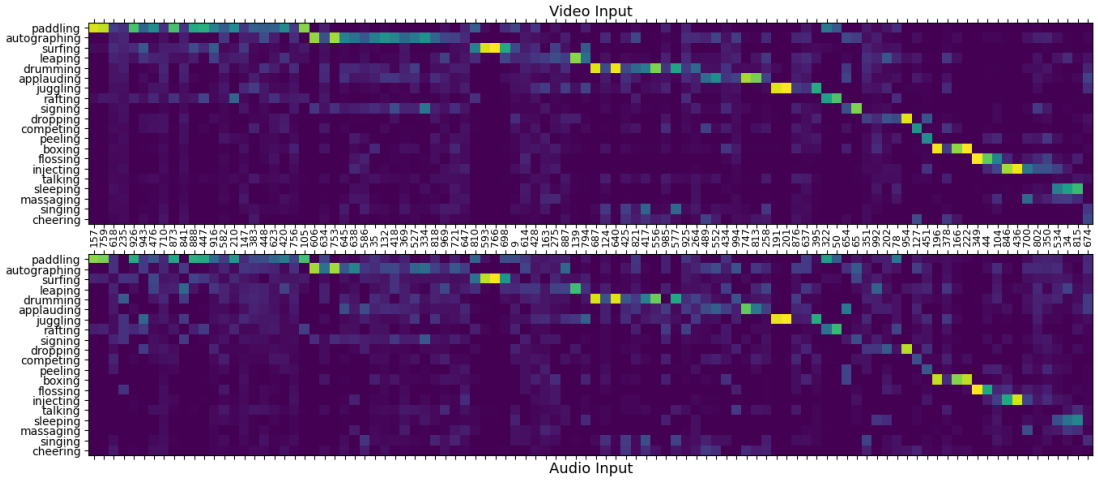

Figure 3: Conditional probability matrix illustrating $P(\text{action}|\text{codeword})$ on the S-MiT development set. Y-axis is action label, showing only the top 20 most frequent labels for simplicity. X-axis is the indices of the top 100 most frequent codewords.

Video-Text: MSR-VTT (Xu et al., 2016) contains 10k video clips with length varying from 10 to 32 seconds. While each video is provided with 20 related captions for training, we followed the evaluation protocol from previous works (Luo et al., 2021; Gabeur et al., 2020; Yu et al., 2018) to use the `training-9k` / `test 1k-A` splits for training and testing respectively. CLIP4Clip (Luo et al., 2021), the current state-of-the-art on MSR-VTT, is selected as the baseline model. Following the cross-modal learning paradigm described in Section 2.1, CLIP4Clip is composed of a pair of encoders: a Visual Transformer (Dosovitskiy et al., 2020) and a Text Transformer (Vaswani et al., 2017). Both encoders are initialized from the CLIP model (Radford et al., 2021), which is pre-trained on the text-image dataset WIT (Radford et al., 2021) and optimized in the end-to-end manner from pixel/text input. For training the proposed framework on top of CLIP4Clip, we freeze the transformers from CLIP4Clip and update only the modules related to the discrete shared embedding space. Both the projection network f^M and the encoder network f^M_{code} are 4D-Convolutions for video with a depth of 3 and BiLSTMs for text, also with a depth of 3. While CLIP4Clip provided different options for the high-level visual encoder f^M_{high}, we adopted the vanilla mean-pooling model. Following CLIP4Clip, the shared embedding space has a dimension of 512.

4.2 Cross-Modal Retrieval

Data retrieval is one of the most common evaluations for cross-modal representation learning. For example, in video retrieval with input query text, videos in the search space will be ranked by the similarity between the representation of each video and the query. We report the standard retrieval metrics recall at rank K (R@K) and median rank (MdR) in Table 1. We show the performance on both visual retrieval, where input language queries are used to retrieve videos or images, and language retrieval, where input visual queries are used to retrieve spoken or text captions.

Video-Audio Retrieval. Video-Audio retrieval on S-MiT (Monfort et al., 2021) is a challenging task since videos are paired with raw speech audio, which is untranscribed, unsegmented, and can contain background noise and speaker variation. However, our proposed framework that leverages cross-modal connections between visual actions and spoken words is able to improve the baseline model by a margin. We further analyze our framework's ability to relate visual actions and spoken words in Section 4.3.

Image-Audio Retrieval. Comparing the baseline model, ResDAVEnet (Harwath et al., 2018), and the current state-of-the-art ResDAVEnet-VQ (Harwath et al., 2020), the latter model introduces VQ units into the audio encoder, allowing it to model the hierarchical structure of speech and achieve better retrieval results. With our framework, we introduce our shared VQ embedding space into the ResDAVEnet model to capture cross-modal interactions. This improves the performance over both ResDAVEnet and ResDAVEnet-VQ.

Video-Text Retrieval. On the benchmark MSR-VTT dataset, we compared our proposed

Table 2: Correspondence between codewords, visual actions, and spoken words. Ranking is based on the precision (Prc.) of the top hypothesis of the visual action label. Occurrence (Occ.) indicates the number of times the codeword was activated throughout the development set. Around 750 codewords were activated on the development set. An extended table is available in Section G of the Appendix.

Rank	Code	Occ.	Visual Action				Spoken word			
			Top Hypothesis		Second Hypothesis		Top Hypothesis		Second Hypothesis	
			Label	Prc.	Label	Prc.	Word	F1	Word	F1
1	201	147	juggling	97.5	kicking	1.2	juggling	36.7	juggles	8.3
2	349	112	flossing	96.0	licking	0.7	floss	15.8	flossing	14.0
3	145	49	surfing	95.6	snowing	2.9	surfboard	23.7	waves	7.3
4	29	64	tattooing	94.6	injecting	2.2	tattoo	15.8	tattooed	4.2
5	233	25	ironing	93.8	hammering	6.2	ironing	20.5	iron	4.7
					...					
32	500	89	dialing	60.0	texting	10.0	dialing	13.8	phone	9.8
33	536	28	cheering	60.0	shouting	10.0	cheerleaders	26.8	cheerleading	10.3
34	50	203	rafting	58.6	paddling	25.7	rafting	16.7	raft	8.5
35	664	78	dunking	58.0	leaping	9.1	basketball	11.0	dunking	5.2
					...					
742	733	188	discussing	6.5	applauding	4.6	men	7.3	two	6.4
743	542	58	baking	6.5	peeling	5.2	cupcake	9.2	peanut	6.2

(a) codeword # 201 (b) codeword # 664

Figure 4: Codeword cross-modal localization. Input regions that are encoded by the codeword (selected from Table 2) are highlighted in red.

method against recent works achieving state-of-the-art (Bain et al., 2021; Liu et al., 2021; Luo et al., 2021) and provide a full comparison against more prior work (Liu et al., 2019b; Rouditchenko et al., 2020; Gabeur et al., 2020; Patrick et al., 2020; Dzabraev et al., 2021; Croitoru et al., 2021) in Section E of the Appendix. Frozen-in-Time (Bain et al., 2021) and CLIP4Clip (Luo et al., 2021) are similar methods that employ a Visual Transformer (Dosovitskiy et al., 2020) to encode video as sequence of images. The key differences between them is the choice of summarizing function (i.e. f^M_{high}) for video and the pre-training procedure. We also note that the CLIP4Clip with tight transformer encoder (Luo et al., 2021) (CLIP4Clip-tightT) relied on cross-modal reference via self-attention encoders to derive representations, which has a higher time complexity as mentioned in Section 3. With the shared codebook and Cross-Modal Code Matching objection, our proposed framework also enables cross-modal reference and gives an improvement over the baseline model without increasing the time complexity.

Overall, our proposed method enables consistent improvements regardless of the data modalities and baseline architectures, demonstrating its effectiveness and generalizability.

4.3 Discrete Representation Analysis

One of the important motivations of introducing the discrete cross-modal embedding space is better model interpretability. In this section, we take a closer look into the codewords learned through our proposed framework. For the evaluation, we chose the video-audio setup on S-MiT (Monfort et al., 2021). We used video-audio pairs from the development set, where each pair is labeled with an action out of 332 categories. Note that we only

used labels for analysis, labels are never used for training.

Conditional Probability of Action Labels Given Codeword. First, we compute the conditional probability distributions of action labels given the codewords over the video inputs. Each video input is fixed-length and represented by 27 codewords (3 frames each represented by 3×3 codewords), and we labeled all these codewords with the video's action label. By accumulating codeword labels through the whole development set, we can compute the conditional probability of each action given any codeword, i.e. $P(\text{action}|\text{codeword})$. Results are visualized in the upper part of Figure 3. Similarly, we computed the conditional probabilities based on the audio input where each utterance is represented by up to 32 codewords depending on the utterance length. We selected the most frequent codewords used by the video inputs and plot the conditional probabilities based on the audio input in the lower part of Figure 3. We can observe that both matrices have similar patterns, i.e., when a codeword is activated, there is a high chance of a specific action appearing in the input regardless if it is video or audio. This suggests that our model is able to learn cross-modal representations for actions grounded by either visual or spoken language input. The codewords are not only modality invariant, but more importantly, they also capture the semantic relations of the labels. e.g., codewords with the highest chance to represent "autographing" typically have the second highest chance of representing "signing"; codewords for "surfing" are less likely to represent other actions as all of them are very different from "surfing". We also note that without the Cross-Modal Code Matching objective, semantically related video and audio inputs no longer use the same codewords, which we illustrate in Section F of the Appendix.

Cross-Modal Correspondences. Next, we analyze the connections captured by the codewords between action labels and spoken words. With the same label accumulation method described previously, we compute the precision of action prediction with codewords (i.e. $\frac{\text{code-action co-occurrence}}{\text{code occurrence}}$). For the audio, we used word-level transcriptions (from Google's speech-to-text API) to assign a spoken word to each codeword when it is activated by the input utterance. This results in a hypothesis set including around 7k words for each codeword, and we listed the top 2 hypotheses for each codeword with the highest F1 score (instead of precision to avoid domination of high-frequency words). Results are listed in Table 2. For the codewords that have the highest precision on predicting the action label, we found the top hypotheses for spoken words are often the action label itself. E.g., the codeword (rank 1st) for the visual action "juggling" maps to the spoken word "juggling" perfectly. As precision on visual action prediction decreases, we observed fewer perfect mappings, but the spoken word hypotheses remained semantically related to the visual action hypotheses. E.g., the codeword (rank 35th) for the visual action "dunking" with lower precision now maps to the spoken word "basketball." Surprisingly, even the codewords with the lowest precision capture relationships between visual actions and spoken words to some extent. E.g., codeword (rank 743th) that is most related to the action "baking" has the top and second word hypotheses "cupcake" and "peanut."

Codeword Localization. Finally, to visualize the relation between codewords and the input data, we localize the segments of both the video and audio input that are assigned to certain codewords. This is possible because quantization in our shared embedding space is done at the fine-grained level, so that the time and spatial axes are preserved. Examples are shown in Figure 4, where the regions assigned to the given code are highlighted. Interestingly, we see the codewords being aligned to both the visual actions and the corresponding spoken words. This supports our claim of having a more interpretable representation at the fine-grained level.

5 Conclusion

In this paper, we proposed a framework for cross-modal representation learning with a discrete embedding space that is shared amongst different modalities and enables model interpretability. We also propose a Cross-Modal Code Matching objective that encourages models to represent cross-model semantic concepts in the embedding space. Combining our discrete embedding space and objective with existing cross-modal representation learning models improves retrieval performance on video-text, video-audio, and image-audio datasets. We also analyze the shared embedding space and find that semantically related video and audio inputs tend to use the same codewords.

Acknowledgements

This research was supported in part by the MIT-IBM Watson AI Lab and its member companies, Nexplore and Woodside, and by MIT Lincoln Laboratory.

References

Jean-Baptiste Alayrac, Adrià Recasens, Rosalia Schneider, Relja Arandjelović, Jason Ramapuram, Jeffrey De Fauw, Lucas Smaira, Sander Dieleman, and Andrew Zisserman. 2020. Self-supervised multimodal versatile networks. *arXiv preprint arXiv:2006.16228*.

Max Bain, Arsha Nagrani, Gül Varol, and Andrew Zisserman. 2021. Frozen in time: A joint video and image encoder for end-to-end retrieval. *arXiv preprint arXiv:2104.00650*.

Yoshua Bengio, Nicholas Léonard, and Aaron Courville. 2013. Estimating or propagating gradients through stochastic neurons for conditional computation. *arXiv preprint arXiv:1308.3432*.

Angie W Boggust, Kartik Audhkhasi, Dhiraj Joshi, David Harwath, Samuel Thomas, Rogério Schmidt Feris, Danny Gutfreund, Yang Zhang, Antonio Torralba, Michael Picheny, et al. 2019. Grounding spoken words in unlabeled video. In *CVPR Workshops*.

Ioana Croitoru, Simion-Vlad Bogolin, Yang Liu, Samuel Albanie, Marius Leordeanu, Hailin Jin, and Andrew Zisserman. 2021. Teachtext: Crossmodal generalized distillation for text-video retrieval. *arXiv preprint arXiv:2104.08271*.

Yann N Dauphin, Angela Fan, Michael Auli, and David Grangier. 2017. Language modeling with gated convolutional networks. In *International conference on machine learning*, pages 933–941. PMLR.

Jia Deng, Wei Dong, Richard Socher, Li-Jia Li, Kai Li, and Li Fei-Fei. 2009. Imagenet: A large-scale hierarchical image database. In *2009 IEEE conference on computer vision and pattern recognition*, pages 248–255. Ieee.

Alexey Dosovitskiy, Lucas Beyer, Alexander Kolesnikov, Dirk Weissenborn, Xiaohua Zhai, Thomas Unterthiner, Mostafa Dehghani, Matthias Minderer, Georg Heigold, Sylvain Gelly, et al. 2020. An image is worth 16x16 words: Transformers for image recognition at scale. *arXiv preprint arXiv:2010.11929*.

Maksim Dzabraev, Maksim Kalashnikov, Stepan Komkov, and Aleksandr Petiushko. 2021. Mdmmt: Multidomain multimodal transformer for video retrieval. *arXiv preprint arXiv:2103.10699*.

Valentin Gabeur, Chen Sun, Karteek Alahari, and Cordelia Schmid. 2020. Multi-modal transformer for video retrieval. In *European Conference on Computer Vision (ECCV)*, volume 5. Springer.

Yaroslav Ganin and Victor Lempitsky. 2015. Unsupervised domain adaptation by backpropagation. In *International conference on machine learning*, pages 1180–1189. PMLR.

Michael Gutmann and Aapo Hyvärinen. 2010. Noise-contrastive estimation: A new estimation principle for unnormalized statistical models. In *Proceedings of the Thirteenth International Conference on Artificial Intelligence and Statistics*, volume 9 of *Proceedings of Machine Learning Research*, pages 297–304, Chia Laguna Resort, Sardinia, Italy. PMLR.

David Harwath and James Glass. 2015. Deep multimodal semantic embeddings for speech and images. In *2015 IEEE Workshop on Automatic Speech Recognition and Understanding (ASRU)*, pages 237–244. IEEE.

David Harwath and James R Glass. 2017. Learning word-like units from joint audio-visual analysis. *arXiv preprint arXiv:1701.07481*.

David Harwath, Wei-Ning Hsu, and James Glass. 2020. Learning hierarchical discrete linguistic units from visually-grounded speech. In *International Conference on Learning Representations*.

David Harwath, Adria Recasens, Dídac Surís, Galen Chuang, Antonio Torralba, and James Glass. 2018. Jointly discovering visual objects and spoken words from raw sensory input. In *Proceedings of the European conference on computer vision (ECCV)*, pages 649–665.

David Harwath, Antonio Torralba, and James R Glass. 2017. Unsupervised learning of spoken language with visual context. In *Neural Information Processing Systems*.

Kaiming He, Xiangyu Zhang, Shaoqing Ren, and Jian Sun. 2016. Deep residual learning for image recognition. In *Proceedings of the IEEE Conference on Computer Vision and Pattern Recognition (CVPR)*.

Gabriel Ilharco, Yuan Zhang, and Jason Baldridge. 2019. Large-scale representation learning from visually grounded untranscribed speech. *arXiv preprint arXiv:1909.08782*.

Herman Kamper, Gregory Shakhnarovich, and Karen Livescu. 2018. Semantic speech retrieval with a visually grounded model of untranscribed speech. In *Proceedings of the IEEE Conference on Computer Vision and Pattern Recognition Workshops*, pages 2514–2517.

Diederik P Kingma and Max Welling. 2013. Auto-encoding variational bayes. *arXiv preprint arXiv:1312.6114*.

Jie Lei, Linjie Li, Luowei Zhou, Zhe Gan, Tamara L Berg, Mohit Bansal, and Jingjing Liu. 2021. Less is more: Clipbert for video-and-language learning via sparse sampling. *arXiv preprint arXiv:2102.06183*.

Ji Lin, Chuang Gan, and Song Han. 2019. Tsm: Temporal shift module for efficient video understanding. In *Proceedings of the IEEE/CVF International Conference on Computer Vision*, pages 7083–7093.

Song Liu, Haoqi Fan, Shengsheng Qian, Yiru Chen, Wenkui Ding, and Zhongyuan Wang. 2021. Hit: Hierarchical transformer with momentum contrast for video-text retrieval. *arXiv preprint arXiv:2103.15049*.

Xihui Liu, Zihao Wang, Jing Shao, Xiaogang Wang, and Hongsheng Li. 2019a. Improving referring expression grounding with cross-modal attention-guided erasing. In *Proceedings of the IEEE/CVF Conference on Computer Vision and Pattern Recognition (CVPR)*.

Yang Liu, Samuel Albanie, Arsha Nagrani, and Andrew Zisserman. 2019b. Use what you have: Video retrieval using representations from collaborative experts. *arXiv preprint arXiv:1907.13487*.

Huaishao Luo, Lei Ji, Ming Zhong, Yang Chen, Wen Lei, Nan Duan, and Tianrui Li. 2021. Clip4clip: An empirical study of clip for end to end video clip retrieval. *arXiv preprint arXiv:2104.08860*.

Antoine Miech, Jean-Baptiste Alayrac, Lucas Smaira, Ivan Laptev, Josef Sivic, and Andrew Zisserman. 2020. End-to-end learning of visual representations from uncurated instructional videos. In *Proceedings of the IEEE/CVF Conference on Computer Vision and Pattern Recognition*, pages 9879–9889.

Antoine Miech, Ivan Laptev, and Josef Sivic. 2018. Learning a text-video embedding from incomplete and heterogeneous data. *arXiv preprint arXiv:1804.02516*.

Antoine Miech, Dimitri Zhukov, Jean-Baptiste Alayrac, Makarand Tapaswi, Ivan Laptev, and Josef Sivic. 2019. Howto100m: Learning a text-video embedding by watching hundred million narrated video clips. In *Proceedings of the IEEE/CVF International Conference on Computer Vision*, pages 2630–2640.

Mathew Monfort, SouYoung Jin, Alexander Liu, David Harwath, Rogerio Feris, James Glass, and Aude Oliva. 2021. Spoken moments: Learning joint audio-visual representations from video descriptions. *arXiv preprint arXiv:2105.04489*.

Mathew Monfort, Kandan Ramakrishnan, Alex Andonian, Barry A McNamara, Alex Lascelles, Bowen Pan, Quanfu Fan, Dan Gutfreund, Rogerio Feris, and Aude Oliva. 2019. Multi-moments in time: Learning and interpreting models for multi-action video understanding. *arXiv preprint arXiv:1911.00232*.

Aaron van den Oord, Yazhe Li, and Oriol Vinyals. 2018. Representation learning with contrastive predictive coding. *arXiv preprint arXiv:1807.03748*.

Aaron van den Oord, Oriol Vinyals, and Koray Kavukcuoglu. 2017. Neural discrete representation learning. *arXiv preprint arXiv:1711.00937*.

Mandela Patrick, Po-Yao Huang, Yuki Asano, Florian Metze, Alexander Hauptmann, João Henriques, and Andrea Vedaldi. 2020. Support-set bottlenecks for video-text representation learning. *arXiv preprint arXiv:2010.02824*.

Alec Radford, Jong Wook Kim, Chris Hallacy, Aditya Ramesh, Gabriel Goh, Sandhini Agarwal, Girish Sastry, Amanda Askell, Pamela Mishkin, Jack Clark, et al. 2021. Learning transferable visual models from natural language supervision. *arXiv preprint arXiv:2103.00020*.

Alec Radford, Jeffrey Wu, Rewon Child, David Luan, Dario Amodei, and Ilya Sutskever. 2019. Language models are unsupervised multitask learners. *OpenAI blog*, 1(8):9.

Andrew Rouditchenko, Angie Boggust, David Harwath, Brian Chen, Dhiraj Joshi, Samuel Thomas, Kartik Audhkhasi, Hilde Kuehne, Rameswar Panda, Rogerio Feris, et al. 2020. Avlnet: Learning audio-visual language representations from instructional videos. *arXiv preprint arXiv:2006.09199*.

Florian Schroff, Dmitry Kalenichenko, and James Philbin. 2015. Facenet: A unified embedding for face recognition and clustering. In *Proceedings of the IEEE conference on computer vision and pattern recognition*, pages 815–823.

Gabriel Synnaeve, Maarten Versteegh, and Emmanuel Dupoux. 2014. Learning words from images and speech. In *NIPS Workshop Learn. Semantics*. Citeseer.

Ashish Vaswani, Noam Shazeer, Niki Parmar, Jakob Uszkoreit, Llion Jones, Aidan N Gomez, Lukasz Kaiser, and Illia Polosukhin. 2017. Attention is all you need. *arXiv preprint arXiv:1706.03762*.

Liming Wang and Mark A Hasegawa-Johnson. 2019. Multimodal word discovery and retrieval with phone sequence and image concepts. In *INTERSPEECH*.

Jun Xu, Tao Mei, Ting Yao, and Yong Rui. 2016. Msr-vtt: A large video description dataset for bridging video and language. In *Proceedings of the IEEE conference on computer vision and pattern recognition*, pages 5288–5296.

Youngjae Yu, Jongseok Kim, and Gunhee Kim. 2018. A joint sequence fusion model for video question answering and retrieval. In *Proceedings of the European Conference on Computer Vision (ECCV)*, pages 471–487.

Bolei Zhou, Agata Lapedriza, Jianxiong Xiao, Antonio Torralba, and Aude Oliva. 2014. Learning deep features for scene recognition using places database. In *NeurIPS*.

Appendix

A Codebook Update Policy

The codebook with d-dimensional codewords is initialized with

$$\begin{aligned} N_v^{(0)} &= 1 \\ m_v^{(0)} &\sim \mathcal{N}_d(0, 1) \\ e_v^{(0)} &= m_v^{(0)}, \end{aligned} \tag{3}$$

and updated with each codeword e_v being the exponential moving average (EMA) of all the fine-grained representations $H = \left\{ f^M(h_{i,l}^M) \;\middle|\; \bar{h}_{i,l}^M = e_v \right\}$ that was replaced by e_v for every training step t:

$$\begin{aligned} N_v^{(t)} &\leftarrow \gamma\, N_v^{(t-1)} + (1-\gamma)\; |H| \\ m_v^{(t)} &\leftarrow \gamma\, m_v^{(t-1)} + (1-\gamma) \sum_{h \in H} h \\ e_v^{(t)} &\leftarrow \frac{m_v^{(t)}}{N_v^{(t)}}, \end{aligned} \tag{4}$$

where the decay factor γ is set to 0.99 throughout this work. To improve the overall usage of the codebook, the input fine-grained representations are modality-wise batch normalized. In addition, codewords that are not activated (i.e. $|H| = 0$) for 100 consecutive steps are re-initialized during codebook update. The reset value is randomly chosen from activated codewords.

B Implementation Details

For each dataset and modality pair considered in this work, we selected baseline models that follow the cross-modal learning paradigm (as described in Section 2.1). Baseline models with different fine-grained and high-level encoders (f_{fine}^M and f_{high}^M) are summarized in Table 3. The links to the official implementation of these baseline models are also provided in the table. For a fair comparison, we retrained the models with the $\mathcal{L}_{\text{MMS}}$ (margin set to 1e-3) as our baseline models.

S-MiT. The input audio feature is a 40 dimensional mel-spectrogram with a window size of 25 ms and a hop size of 10 ms. The baseline is trained with a batch size of 2048 and a learning rate of 1e-3. To train the shared discrete embedding space, we warm-started from the baseline model with a learning rate of 1e-4. Each video is encoded into 27 codewords ($3 \times 3 \times 3$ for time, height, width) and every 16 consecutive frames from the spectrogram is encoded into 1 codeword. The baseline model is trained for 4 hours on 4 V100 GPUs; and it takes an additional 1 hour to train the proposed framework. For both baseline model and our proposed model, we followed the previous work (Monfort et al., 2021) to perform a second round training with a learning rate of 1e-5 and a batch size of 128. The second round training fine-tunes the TSM video encoder (which is frozen in the first round training) on S-MiT jointly with the rest of the components, which takes 2 days on 8 Titan RTX GPUs.

Places. The input audio feature is a 40 dimentional mel-spectrogram with a window size of 25 ms and a hop size of 10 ms. The baseline is trained with a batch size of 256 and a learning rate of 1e-3. To train the shared discrete embedding space, we warm-started from the baseline model with a learning rate of 1e-4. Each image is encoded into 49 codewords (7×7 for height, width) and every 16 consecutive frames from the spectrogram is encoded into 1 codeword. The baseline model is trained for 36 hours on 1 V100 GPU; and it takes an additional 4 hours to train the proposed framework.

MSR-VTT. For our baseline model, we did not reproduce CLIP4Clip's post-pretraining stage, which trained CLIP4Clip on the subset of HowTo100M (Miech et al., 2019) before adapting to MSR-VTT, since this stage is not necessary for the best results on MSR-VTT and the subset is not released. We used all of the hyper-parameters of the official implementation except the batch size is reduced from 128 to 64 to meet our hardware restriction. To train the shared discrete embedding space, we warm-started from the baseline model with a learning rate of 1e-5. Each video is encoded into 8 codewords ($2 \times 2 \times 2$ for time, height, width) and each subword unit in the sentence is encoded into 1 codeword. The baseline model is trained for 12 hours on 8 2080Ti GPUs; and it takes an additional 6 hours to train the proposed framework.

C Ablation Study

To justify our framework design and choice of hyperparameters, we conducted an ablation study on the image-audio setting and report the results in Table 4.

Impact of the shared embedding space. For the codebook size, 1024 codewords worked well across different datasets. Halving and doubling the number of codewords (row(b) & (c)) both decreased

Table 3: Experiment setup on S-MiT, Places, and MSR-VTT.

Setup	Modality	Encoders from baseline model	
Dataset	A	f^A_{fine}	f^A_{high}
- Baseline model	B	f^B_{fine}	f^B_{high}
S-MiT (Monfort et al., 2021)	video	ResNet-152[4] (He et al., 2016) + TSM[5] (Lin et al., 2019)	Max Pooling + GLU (Dauphin et al., 2017)
- AVLnet (Rouditchenko et al., 2020)	audio	Spectrogram+1D-ResNet (Harwath et al., 2018)	Avg. Pooling + GLU (Dauphin et al., 2017)
Places (Harwath et al., 2017)	image	ResNet-50[4] (He et al., 2016)	Avg. Pooling + GLU (Dauphin et al., 2017)
- ResDAVEnet[2] (Harwath et al., 2018)	audio	Spectrogram+1D-ResNet (Harwath et al., 2018)	Avg. Pooling + GLU (Dauphin et al., 2017)
MSR-VTT (Xu et al., 2016)	video	Vision Transformer[3] (Dosovitskiy et al., 2020)	Avg. Pooling + Linear
- CLIP4Clip[1] (Luo et al., 2021)	text	Transformer[3] (Vaswani et al., 2017; Radford et al., 2019)	`[EOT]` token + Linear

[1] https://github.com/ArrowLuo/CLIP4Clip
[2] https://github.com/wnhsu/ResDAVEnet-VQ (under BSD license)
[3] Initialized from CLIP model pretrained on WebImageText dataset (Radford et al., 2021).
[4] Pretrained on ImageNet (Deng et al., 2009).
[5] Pretrained on Multi-MiT (Monfort et al., 2019).

Table 4: Ablation study on Places (Harwath et al., 2017), scores are averaged over audio and image retrieval.

Method	Averaged 2-way Retrieval			
	R@1 ↑	R@5 ↑	R@10 ↑	MnR ↓
(a) Proposed	46.0	77.6	85.9	11.3
(b) codebook size = 512	46.2	77.4	85.2	11.5
(c) codebook size = 2048	46.1	76.6	84.7	12.1
(d) $\alpha = 1.0$	45.6	76.6	85.5	11.6
(e) $\alpha = 0.0$ (w/o CMCM)	45.2	75.5	84.2	12.8
(f) w/o VQ & w/o CMCM	45.7	75.9	84.7	12.6
(g) w/o warm-start	41.6	73.4	82.5	16.0
(h) w/o cont. repr. ($f^M_{\text{high}}(H^M_i)$)	29.0	63.0	74.7	19.4
(i) Our Baseline	42.1	73.7	82.5	13.4

the performance slightly. For the weight α of the proposed Cross-Modal Code Matching objective, we found that values in the range $(0, 1]$ generally work while 0.1 works the best (row(a) v.s. row(d)). Removing the proposed Cross-Modal Code Matching objective (setting $\alpha = 0$, row(e)), however, hurts the performance. Furthermore, without the objective, the codebook no longer captures cross-modal correspondences, as illustrated in Section F of the Appendix. We also observed that disabling the VQ layer together with the Cross-Modal Code Matching objective slightly recovers performance (row(f) v.s. row(e)). All of these observations serve as evidence that the proposed discrete embedding space is most beneficial to the retrieval task with the guidance from the Cross-Modal Code Matching objective.

Importance of baseline models in the cross-modal learning paradigm. As mentioned in Section 4.1, the discrete shared embedding space is learned with "warm-starting" from a baseline model. We note that warm-starting is important for getting more refined representations that yield better retrieval results (row(a) v.s. row(g)). Without warm-starting, our framework can only perform similar to the baseline (row(g) v.s. row(i)). This finding aligns with previous work (Harwath et al., 2020) that used VQ layers in the audio encoder and used warm-starting to learn acoustic units. Moreover, removing the continuous representations (row(h)) originally used in the cross-modal learning paradigm and using only the codeword representations significantly decreases performance. This exposes the trade-off between interpretability and end-task performance by imposing a discrete embedding space. Hence, we choose to integrate both discrete and continuous embedding space for retrieval.

D Failure Attempts with Possible Alternatives

As shown in our experiments and ablation study, the key to improve model interpretability and high-level retrieval performance by our proposed method is learning *domain-invariant* discrete representation. To show the necessity of the proposed Cross-Modal Code Matching, we also provide a list of methods we already tried but failed that eventually helped us derive domain-invariant representation with the proposed Cross-Modal Code Matching:

1. Domain adversarial training over continuous representation

   Domain adversarial training is a common technique to learn domain-invariant representation. The method introduces an auxiliary classifier to classify the source domain of the representation in the latent space. To train domain-invariant encoders (f^M_{fine}), a gradient reversal layer (Ganin and Lempitsky, 2015) is introduced between the classifier and the encoder and the whole system is trained in an end-to-end manner. In practice, this method

results in mode collapse at the fine-grained representation level, i.e., the model neglects input and produces a constant vector. This leads to adding noise with small variance to the high-level representation and results in slightly worse retrieval scores.

2. Domain adversarial training over distribution over codebook

   As an alternative, domain adversarial training can also be performed in the discrete embedding space. In practice, we observed code collapse at the fine-grained representation level, i.e., only 1 codeword is active out of the entire codebook. This leads to adding constant noise to the high-level representation.

3. VAE-like prior distribution regularization over continuous representation

   Another common technique to enforce domain-invariant latent space is to adapt identical prior distributions over representation from different domains. This can be implemented by adding a regularization term during training which minimizes the KL-divergence between representation from model and the desired prior distribution as shown in Variational Auto-Encoder (Kingma and Welling, 2013). In practice, we tried both Gaussian and uniform prior, and both resulted in mode collapse, similar to method 1.

4. VAE-like Prior distribution regularization over distribution over codebook

   With the distribution over codebook defined in Section 2.3, we can also adapt prior distribution regularization in the discrete latent space instead of the continuous space. However, we observed code collapse where only certain codewords will be utilized by the model in our experiments, similar to method 2.

5. Minimizing the cross-entropy/JSD/KLD between distribution over codebook of each positive pair (i.e. no negative sampling in the CMCM loss)

   Besides the proposed Cross-Modal Code Matching , we also experimented with different substitutes that might be able to encourage codeword sharing across domains, including cross-entropy, JS-divergence, and KL-divergence. While cross-entropy leads to code collapse similar to method 2., JSD and KLD lead to uniform code distribution for each input instance, making fine-grained representation uninformative. A possible explanation is that both measurements include the negative entropy term. Minimizing them encourages uniform distribution over the codebook.

Note that **unlike all the objectives above, the proposed Cross-Modal Code Matching loss not only enforces the model to learn domain-invariant representation but also introduces contrastive learning simultaneously.** To be more specific, different view (modality) of the same instance is encouraged to share similar codeword combinations while different instance should be encoded into different codeword combinations. This key difference allows our method to learn informative discrete codewords that align to the goal of the high-level objective function.

E MSR-VTT Video Retreival Full Comparison

In addition to the comparison against recent state-of-the-art methods in Table 1 for video retrieval on MSR-VTT, in Table 5 we show the complete comparison to prior work and summarize the models here. Collaborative Experts (Liu et al., 2019b) leverages "expert" features that can be obtained from the raw video from different off-the-shelf models (such as object detection, scene classification, and speech recognition models) to build representations. Instead of summarizing the expert features into a compact video representation and computing similarity with the text representation, the Multi-Modal Transformer (Gabeur et al., 2020) computes similarity between different expert features and the text representation with a proposed variation of the Transformer (Vaswani et al., 2017). Based on the Multi-Modal Transformer, Multidomain Multi-Modal Transformer (Dzabraev et al., 2021) explored an additional motion feature and the combination of different training datasets to further improve the result. Support-Set Bottlenecks (Patrick et al., 2020) studies the benefit that cross-instance captioning can bring by generating text based on the combination of all representations of similar videos. Similar to our framework, Hierarchical Transformer with Momentum Contrast (Liu et al., 2021) divided representations from different layer of the encoders into fine-grained (which they referred to feature-level) and high-level

Table 5: Full comparison against prior works on MSR-VTT text-to-video retrieval.

Method	Video Retrieval (Text → Video)			
	R@1 ↑	R@5 ↑	R@10 ↑	MnR ↓
Collaborative Experts (Liu et al., 2019b)	20.9	48.8	62.4	28.2
Multi-Modal Transformer (Gabeur et al., 2020)	26.6	57.1	69.6	24.0
Support-Set Bottlenecks (Patrick et al., 2020)	30.1	58.5	69.3	-
Multidomain Multimodal Transformer (Dzabraev et al., 2021)	38.9	69.0	79.7	16.5
Frozen-in-Time (Bain et al., 2021)	31.0	59.5	70.5	-
Hierarchical Transformer with Momentum Contrast (Liu et al., 2021)	30.7	60.9	73.2	-
TeachText (Croitoru et al., 2021)	29.6	61.6	74.2	-
CLIP4Clip-meanPooling (Luo et al., 2021)	43.1	70.4	80.8	16.2
CLIP4Clip-seqLSTM (Luo et al., 2021)	42.5	70.8	80.7	16.7
CLIP4Clip-seqTransformer (Luo et al., 2021)	44.5	71.4	81.6	15.3
CLIP4Clip-tightTransformer (Luo et al., 2021)	40.2	71.5	80.5	13.4
Our Baseline (based on CLIP4Clip-meanPooling)	42.6	71.2	80.8	15.5
Proposed	43.4	72.3	81.2	14.8

(which they reffered to semantic-level) representations. While our work focused on learning discrete representations in the fine-grained embedding space, they performed momentum-based representation matching across the two levels that encourages the two embedding spaces to be more similar. TeachText (Croitoru et al., 2021) leverages distillation learning where multiple captions describing the same video can be considered by different teacher models that jointly guide the student network. Frozen-in-Time (Bain et al., 2021) and CLIP4Clip (Luo et al., 2021) both found the recent proposed Visual Transformer (Dosovitskiy et al., 2020) can significantly improve retrieval results while they differ in the choice of summarizing function for video (i.e. f^M_{high}) and the pre-training procedure. Moreover, CLIP4Clip also introduces different choice of the summarizing function f^M_{high} including RNNs (CLIP4Clip-seqLSTM) and Transformers (CLIP4Clip-seqTransformer) that replaces the mean-pooling function (CLIP4Clip-meanPooling) at the cost of higher time complexity and computational cost. Note that while our work is based on the vanilla mean-pooling function, we achieved comparable or better performance with the proposed discrete embedding representations. As described in Section 3, CLIP4Clip also introduced a cross-modal transformer network (CLIP4Clip-tightTransformer) that allows cross-modal reference for deriving representations.

F Results Without Cross-Modal Code Matching

To demonstrate the importance of our proposed Cross-Modal Code Matching objective, Figure 5 illustrates the conditional probability matrix (described in Section 4.3 and Figure 3) when the proposed objective is deactived (setting $\alpha = 0$). Unsurprisingly, we see that the correlation between codewords and action labels are gone, indicating that the assignment of codewords are now dominated by the input modality instead of the underlying action label. This can also be verified by visualizing the discrete embedding space in a lower dimension as plotted in Figure 6. This evidence suggests that the proposed Cross-Modal Code Matching Objective is effective for learning modality-invariant representations.

G Additional Codeword Correspondence and Localization Examples

An extension of Table 2 showing the correspondence between codewords, visual actions, and spoken words are provided in Table 6. We also provide more examples for codeword localization in Figure 7.

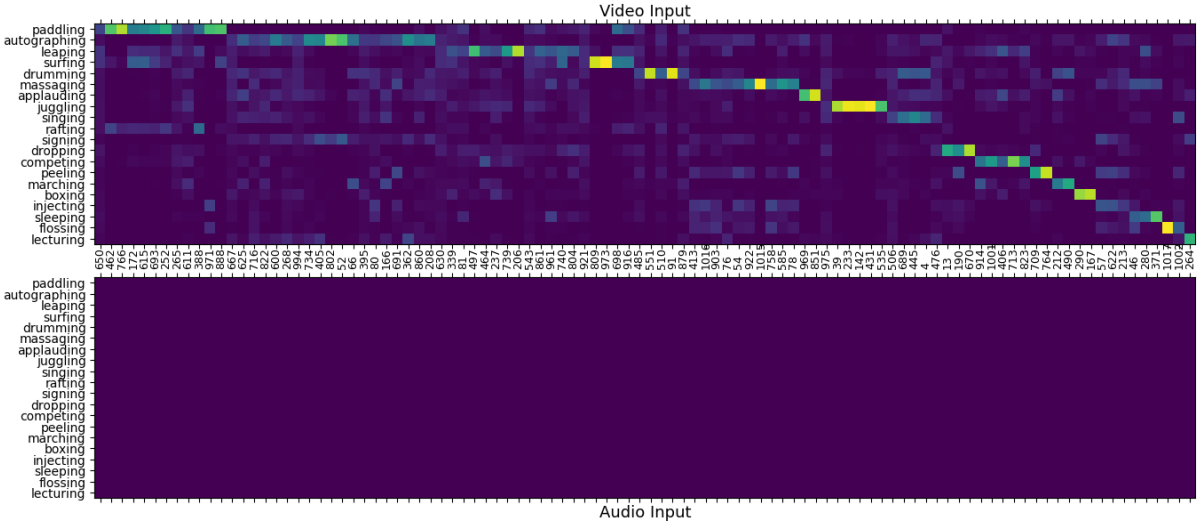

Figure 5: Conditional probability matrix between codewords and action labels learned by our proposed method when the Cross-Modal Code Matching objective is excluded.

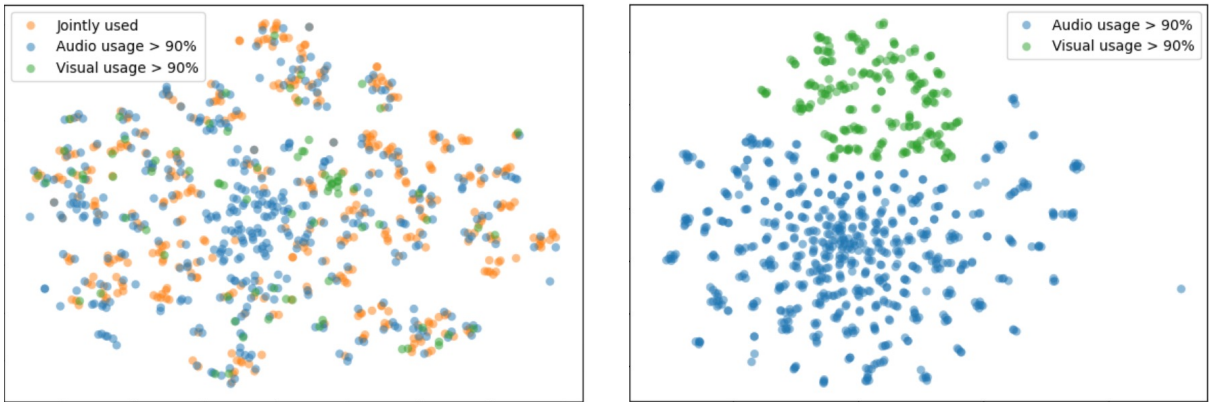

(a) With Cross-modal Code Matching (b) Without Cross-modal Code Matching

Figure 6: T-SNE visualization of the codebook with and without the proposed Cross-Modal Code Matching Objective. Each point corresponds to a codeword colored with respect to the input modality that utilized it the most. Codewords without high ($> 90\%$) usage from single modality are labeled as "jointly used".

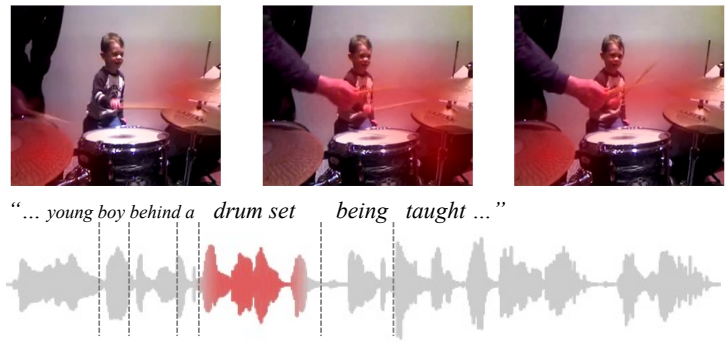

(a) codeword # 687

(b) codeword # 327

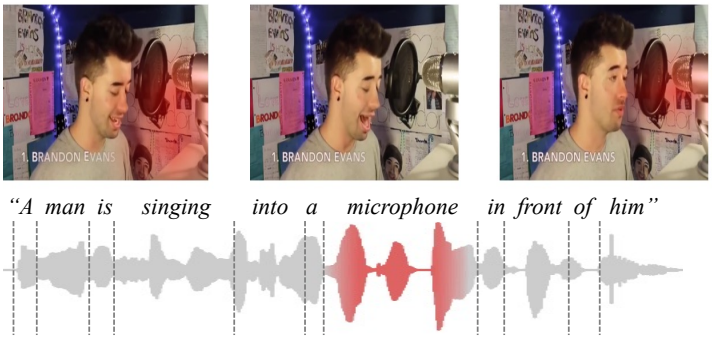

(d) codeword # 36

Figure 7: More examples for codeword cross-modal localization.

Table 6: Correspondence between codewords, visual actions, and spoken words (Extended Table 2). The second hypothesis and the occurrence are omitted for simplicity. All codewords activated on S-MiT's development set are listed.

Rank	Code	Visual Action Top Hypothesis		Spoken word Top Hypothesis		Rank	Code	Visual Action Top Hypothesis		Spoken word Top Hypothesis	
		label	Prc.	word	F1			label	Prc.	word	F1
1	201	juggling	97.5	juggling	36.7	61	940	landing	44.9	airplane	19.6
2	349	flossing	96.0	floss	15.8	62	262	sewing	44.7	sewing	13.2
3	145	surfing	95.6	surfboard	23.7	63	532	autographing	44.4	selfie	22.2
4	29	tattooing	94.6	tattoo	15.8	64	928	stirring	44.1	boiling	27.3
5	233	ironing	93.8	ironing	20.5	65	747	applauding	43.8	clapping	23.8
6	766	surfing	93.2	surfing	22.1	66	447	paddling	43.1	boat	8.3
7	191	juggling	90.2	juggling	29.1	67	823	skipping	43.0	jump	17.1
8	753	autographing	85.0	autographs	26.4	68	308	shaving	42.5	comb	10.0
9	606	autographing	83.7	signing	16.2	69	518	skiing	41.8	skiing	11.4
10	640	drumming	81.6	drums	19.5	70	860	bulldozing	41.7	bulldozer	25.7
11	436	injecting	81.6	injected	13.2	71	61	extinguishing	41.3	sting	9.1
12	109	peeling	80.9	peeling	21.2	72	296	combing	40.9	brushes	5.9
13	551	shaving	80.2	shaving	18.0	73	435	screwing	40.8	drill	25.0
14	137	paddling	80.0	canoe	25.8	74	705	surfing	40.6	ocean	27.0
15	327	crying	78.8	crying	29.5	75	760	hammering	40.0	hammering	23.3
16	593	surfing	77.7	surfboard	10.9	76	926	paddling	40.0	lake	6.8
17	687	drumming	77.3	drums	14.4	77	888	paddling	39.6	lake	7.4
18	883	tattooing	77.2	tattoo	13.6	78	169	dunking	39.3	nba	7.5
19	1000	inflating	74.5	inflatable	12.8	79	681	manicuring	38.7	nails	13.2
20	222	boxing	71.3	boxing	13.2	80	685	signing	38.6	writing	8.3
21	243	shredding	70.0	shredding	28.6	81	631	paddling	38.5	clouds	12.2
22	157	paddling	69.9	kayak	21.3	82	800	dropping	38.3	beans	12.9
23	427	boxing	69.8	boxers	16.2	83	556	drumming	38.3	marching	11.6
24	774	surfing	69.2	waves	23.0	84	758	wrapping	38.1	wrapping	22.2
25	613	manicuring	67.9	nails	24.5	85	368	texting	38.0	texting	16.7
26	952	leaping	66.0	dolphins	10.7	86	625	combing	37.9	hair	4.9
27	196	boxing	64.1	boxer	13.9	87	166	boxing	37.8	boxing	7.2
28	706	sailing	63.4	sailboat	18.8	88	539	paddling	37.5	helmet	13.0
29	58	shaving	62.8	shaving	10.9	89	139	leaping	37.5	jumping	16.6
30	759	paddling	60.7	paddling	12.4	90	123	drumming	37.1	playing	8.7
31	868	boxing	60.0	boxer	11.2	91	577	drumming	37.0	musical	8.1
32	500	dialing	60.0	dialing	13.8	92	780	screwing	36.9	drill	15.8
33	536	cheering	60.0	cheerleaders	26.8	93	621	leaping	36.6	jumps	9.7
34	50	rafting	58.6	rafting	16.7	94	154	boxing	36.0	referee	14.7
35	664	dunking	58.0	basketball	11.0	95	415	grilling	35.7	grill	15.7
36	103	autographing	57.8	carpet	8.2	96	345	autographing	35.5	pictures	19.3
37	990	wrestling	56.1	wrestling	25.9	97	694	sailing	34.9	sailing	7.0
38	880	sleeping	56.0	sleeping	21.1	98	973	leaping	34.4	tale	8.0
39	48	paddling	55.1	rowing	18.2	99	957	shrugging	34.4	lifting	10.3
40	292	skiing	54.2	skiing	20.0	100	713	paddling	34.3	sunset	25.3
41	602	ironing	52.5	ironing	7.1	101	697	injecting	34.1	doctor	18.8
42	954	dropping	52.4	dropped	8.2	102	431	peeling	33.9	apple	20.0
43	735	applauding	52.1	clapping	23.4	103	164	typing	33.8	laptop	20.6
44	816	autographing	51.0	carpet	22.5	104	776	juggling	33.6	balls	16.5
45	516	swinging	50.0	swing	20.4	105	73	shrugging	32.9	weight	14.6
46	421	carving	50.0	carving	27.2	106	846	injecting	32.8	gloves	7.8
47	168	drumming	49.3	marching	17.5	107	395	juggling	32.7	balls	10.1
48	561	flossing	48.0	mouse	10.0	108	273	dusting	32.6	clean	11.5
49	970	marrying	47.8	bride	22.2	109	737	paddling	32.5	mountains	14.0
50	610	dunking	47.4	basketball	19.5	110	291	coughing	32.4	sneezes	15.6
51	105	paddling	47.2	river	23.7	111	375	colliding	32.4	crashing	14.5
52	150	waxing	47.2	wax	20.3	112	693	sleeping	32.3	baby	28.9
53	92	howling	46.7	barking	15.1	113	111	baking	32.3	baker	13.8
54	929	typing	46.3	typing	22.4	114	805	massaging	32.0	squatted	8.7
55	844	drumming	46.2	band	14.5	115	134	autographing	31.7	obama	7.5
56	497	cheering	45.8	cheerleaders	34.8	116	923	wrapping	31.6	tape	16.7
57	322	paddling	45.8	kayak	7.2	117	698	surfing	31.5	beach	9.8
58	672	boxing	45.6	fighting	28.8	118	362	paddling	31.5	water	8.2
59	97	barbecuing	45.6	grill	26.4	119	505	drumming	31.0	guitar	13.1
60	216	inflating	45.3	balloon	10.3	120	215	shaving	31.0	vent	12.1

Table 6: continued

Rank	Code	Visual Action Top Hypothesis label	Prc.	Spoken word Top Hypothesis word	F1	Rank	Code	Visual Action Top Hypothesis label	Prc.	Spoken word Top Hypothesis word	F1
121	642	autographing	30.8	sign	9.9	181	646	autographing	23.5	taking	11.6
122	828	paddling	30.6	river	3.6	182	423	applauding	23.5	crowd	11.1
123	6	leaping	30.3	monkey	31.4	183	699	racing	23.4	motorcycle	16.5
124	974	sprinkling	30.0	sprinkler	26.7	184	651	paddling	23.4	sky	4.5
125	44	flossing	29.9	teeth	3.0	185	414	drenching	23.3	rain	16.9
126	342	drumming	29.9	playing	7.7	186	55	racing	23.3	race	12.0
127	108	boxing	29.8	practicing	24.1	187	718	drumming	23.2	costume	9.2
128	784	pedaling	29.7	bikes	13.1	188	439	pedaling	23.1	cyclist	12.6
129	266	barbecuing	29.7	meat	22.5	189	19	clipping	23.1	tractor	22.2
130	991	drumming	29.6	guitar	11.0	190	255	paddling	23.1	water	3.6
131	597	signing	29.3	writing	4.7	191	701	lecturing	23.0	preacher	16.3
132	817	welding	29.1	steel	11.6	192	444	autographing	22.9	protesters	7.4
133	673	typing	29.1	laptop	12.3	193	859	singing	22.9	performer	5.6
134	113	dialing	29.0	telephone	11.7	194	18	applauding	22.9	cheering	16.2
135	470	sawing	28.9	saw	10.5	195	371	barbecuing	22.9	fire	10.1
136	657	landing	28.7	airplane	11.7	196	315	peeling	22.8	orange	19.9
137	440	surfing	28.6	cap	6.1	197	271	racing	22.7	race	11.1
138	404	rinsing	28.6	scrubbing	13.3	198	955	leaping	22.6	seagulls	24.2
139	0	applauding	28.6	protesting	13.8	199	584	boxing	22.6	bag	23.7
140	950	paddling	28.2	water	9.7	200	555	pitching	22.5	baseball	19.6
141	430	hiking	27.8	hikers	13.8	201	286	piloting	22.5	helicopter	12.5
142	762	leaping	27.8	diving	12.0	202	569	paddling	22.3	down	17.6
143	504	bowing	27.3	praying	19.0	203	692	paddling	22.2	train	31.4
144	295	paddling	27.2	bridge	26.4	204	682	paddling	22.1	trees	16.3
145	579	dunking	27.2	ball	10.5	205	116	slicing	22.0	cutting	22.4
146	380	leaping	26.7	deer	29.3	206	442	dropping	22.0	wipers	16.3
147	152	sleeping	26.7	laying	14.3	207	324	skiing	22.0	skis	4.1
148	603	leaping	26.5	slipping	4.7	208	924	flooding	21.9	flooded	16.3
149	838	dusting	26.5	vacuum	14.3	209	826	bulldozing	21.6	tractor	7.0
150	825	scooping	25.9	spilled	16.7	210	422	falling	21.4	waterfall	19.4
151	64	pedaling	25.9	bicycles	8.5	211	931	bulldozing	21.4	bulldozer	18.2
152	455	erupting	25.6	smoke	20.6	212	259	wrestling	21.3	cuddling	8.0
153	429	competing	25.5	field	13.0	213	475	leaping	21.2	dance	6.1
154	989	competing	25.5	football	19.0	214	905	jumping	21.2	horse	29.1
155	223	competing	25.4	soccer	25.0	215	806	jogging	21.2	jogging	14.3
156	51	bowling	25.4	dome	8.2	216	813	applauding	21.1	waving	15.9
157	379	slicing	25.4	slicing	12.2	217	538	paddling	21.0	water	6.7
158	911	paddling	25.4	aerial	28.0	218	101	massaging	20.9	dog	13.5
159	364	leaping	25.4	bed	18.6	219	482	swinging	20.9	swinging	7.9
160	483	paddling	25.3	flowing	5.7	220	680	leaping	20.9	air	24.1
161	634	autographing	25.0	graduation	4.4	221	1018	dialing	20.7	tapping	44.4
162	884	leaping	25.0	trampoline	8.8	222	665	shaving	20.7	hair	4.1
163	485	stirring	25.0	pan	20.3	223	417	drumming	20.6	stage	8.1
164	540	boxing	25.0	jacks	6.7	224	165	mowing	20.6	lawn	16.5
165	13	paddling	25.0	boat	18.1	225	194	flossing	20.6	scoop	6.9
166	873	paddling	25.0	mountains	8.9	226	200	smashing	20.5	smashed	12.2
167	909	autographing	24.3	book	14.0	227	453	carving	20.4	wood	17.5
168	638	autographing	24.3	either	3.3	228	57	child+singing	20.2	singing	18.5
169	963	plugging	24.3	plug	11.8	229	420	paddling	20.0	forest	13.3
170	131	paddling	24.2	yellow	26.5	230	918	massaging	19.8	laying	13.5
171	799	welding	24.2	construction	27.9	231	810	paddling	19.8	dolphin	2.9
172	486	hammering	24.1	hammering	6.0	232	520	sailing	19.7	boats	5.8
173	465	competing	24.0	teams	11.9	233	190	knitting	19.6	string	10.9
174	67	lecturing	24.0	conference	9.8	234	1016	mopping	19.6	mopping	15.1
175	325	texting	24.0	phone	12.7	235	317	dunking	19.4	basket	18.9
176	1001	competing	23.9	soccer	8.1	236	827	paddling	19.3	ski	8.7
177	242	competing	23.9	football	6.7	237	24	leaping	19.2	dancing	10.2
178	714	calling	23.7	telephone	6.7	238	1019	dropping	19.1	falls	12.1
179	89	competing	23.6	soccer	17.7	239	997	sleeping	19.0	baby	8.3
180	1013	paddling	23.5	forest	19.1	240	77	peeling	19.0	makeup	17.0

Table 6: continued

Rank	Code	Visual Action Top Hypothesis label	Prc.	Spoken word Top Hypothesis word	F1	Rank	Code	Visual Action Top Hypothesis label	Prc.	Spoken word Top Hypothesis word	F1
241	126	leaping	18.9	exercising	18.8	301	459	paddling	16.3	view	9.1
242	449	leaping	18.9	tree	17.6	302	323	shaving	16.3	head	19.8
243	187	surfing	18.9	riding	12.3	303	522	dunking	16.3	court	12.5
244	117	raining	18.8	traffic	21.7	304	773	storming	16.2	storm	9.8
245	671	paddling	18.8	city	13.8	305	748	autographing	16.2	sidewalk	14.3
246	736	autographing	18.7	howling	4.9	306	299	punting	16.2	kicks	7.3
247	251	surfing	18.5	scuba	7.0	307	981	paddling	16.2	jacket	14.1
248	491	raining	18.4	simpsons	8.5	308	627	singing	16.2	dark	14.4
249	1	burying	18.4	dirt	19.3	309	239	fishing	16.2	fishing	21.5
250	188	autographing	18.4	beard	8.8	310	41	leaping	16.1	slow	26.0
251	742	pedaling	18.3	bike	22.0	311	479	leaping	16.1	kids	6.8
252	531	chewing	18.2	eats	12.5	312	348	reaching	16.0	slipping	7.7
253	130	applauding	18.1	crowd	7.4	313	63	dropping	16.0	leaves	18.2
254	246	clinging	18.0	bird	31.2	314	892	applauding	16.0	flag	13.6
255	318	dialing	17.9	phone	6.8	315	558	stirring	16.0	cooking	9.9
256	329	extinguishing	17.9	fire	14.5	316	691	paddling	16.0	background	19.0
257	387	barbecuing	17.9	sausages	10.7	317	319	leaping	15.9	up	3.8
258	993	autographing	17.9	movie	7.6	318	845	stirring	15.8	blade	6.7
259	961	paddling	17.9	rushing	8.3	319	801	paddling	15.8	mask	14.7
260	921	surfing	17.8	beach	15.0	320	726	swimming	15.8	swimming	12.2
261	208	cheering	17.8	stadium	15.0	321	458	shrugging	15.8	karate	3.5
262	650	leaping	17.8	jumps	6.4	322	912	applauding	15.7	old	11.0
263	388	dropping	17.8	float	5.6	323	648	peeling	15.7	kitchen	13.8
264	78	paddling	17.8	walnut	6.5	324	572	dialing	15.5	block	3.2
265	332	dropping	17.7	falling	8.8	325	330	paddling	15.5	waterfall	3.3
266	244	lecturing	17.6	giving	7.3	326	211	leaping	15.5	cat	17.9
267	948	paddling	17.6	across	8.9	327	752	paddling	15.5	trail	6.7
268	1008	surfing	17.6	scuba	4.1	328	34	sleeping	15.5	bed	8.6
269	554	sewing	17.6	machine	12.2	329	792	autographing	15.5	sitting	3.5
270	604	leaping	17.6	fish	25.2	330	588	sowing	15.4	farmer	10.5
271	587	saluting	17.5	soldier	12.0	331	869	pouring	15.4	poured	20.5
272	509	discussing	17.5	office	23.5	332	840	leaping	15.4	pool	11.3
273	720	competing	17.5	track	24.2	333	407	measuring	15.4	drawing	8.5
274	1022	shrugging	17.5	gym	18.1	334	667	welding	15.4	metal	17.6
275	987	autographing	17.4	baseball	21.3	335	661	colliding	15.4	hockey	25.0
276	294	drumming	17.4	stick	16.9	336	560	flossing	15.4	animation	14.0
277	552	applauding	17.4	crowd	18.4	337	149	lecturing	15.4	graphs	8.7
278	995	draining	17.4	waterfall	14.3	338	175	autographing	15.3	walking	7.1
279	284	drumming	17.3	concert	29.3	339	815	sleeping	15.3	baby	17.5
280	808	draining	17.3	water	5.8	340	608	autographing	15.3	people	6.1
281	977	snowing	17.2	snowy	10.3	341	795	leaping	15.2	animals	13.6
282	495	unloading	17.1	time-lapse	21.7	342	755	peeling	15.2	kitchen	12.0
283	184	autographing	17.1	hat	16.8	343	138	juggling	15.2	shirtless	18.2
284	210	paddling	17.1	rocks	14.1	344	496	hanging	15.2	hanging	17.9
285	120	boxing	17.0	shorts	13.7	345	641	competing	15.1	marching	4.4
286	914	paddling	17.0	two	8.3	346	2	drumming	15.0	stage	16.7
287	263	dropping	16.9	fruits	8.1	347	916	paddling	15.0	sunny	3.4
288	245	competing	16.9	kicking	7.6	348	393	chewing	15.0	eating	15.4
289	639	autographing	16.8	dress	8.8	349	609	autographing	15.0	talking	2.5
290	739	autographing	16.7	greenfield	9.8	350	269	draining	15.0	water	12.2
291	704	leaping	16.7	dance	15.0	351	731	flossing	15.0	demonstrating	9.0
292	562	splashing	16.7	splashes	19.0	352	513	dialing	14.9	finger	10.0
293	658	splashing	16.7	bottle	24.6	353	382	paddling	14.9	sky	7.0
294	629	sleeping	16.7	reports	14.8	354	645	autographing	14.8	people	3.3
295	1014	massaging	16.6	getting	10.3	355	553	juggling	14.8	spinning	13.8
296	503	pedaling	16.5	jogging	7.2	356	490	spitting	14.8	drink	19.5
297	686	paddling	16.4	nuts	3.6	357	807	crushing	14.7	crushed	13.6
298	734	singing	16.4	singing	15.9	358	412	autographing	14.7	player	9.1
299	334	autographing	16.3	papers	6.8	359	900	leaping	14.7	branch	23.8
300	788	signing	16.3	reading	8.7	360	622	paddling	14.5	rocks	15.9

Table 6: continued

Rank	Code	Visual Action Top Hypothesis		Spoken word Top Hypothesis	
		label	Prc.	word	F1
361	623	paddling	14.5	yellow	8.7
362	462	leaping	14.5	dancing	18.5
363	65	autographing	14.5	pen	5.0
364	480	leaping	14.5	greetings	7.5
365	376	paddling	14.5	large	22.9
366	730	paddling	14.4	camera	7.2
367	213	paddling	14.4	red	16.0
368	460	trimming	14.3	tomatoes	15.8
369	861	dusting	14.3	swiffer	10.0
370	537	leaping	14.3	daughter	15.4
371	933	towing	14.3	truck	26.5
372	636	paddling	14.3	trees	15.9
373	336	juggling	14.2	fire	15.2
374	794	juggling	14.2	boy	3.2
375	283	piloting	14.1	statue	9.4
376	20	singing	14.1	camera	5.8
377	419	leaping	14.0	flying	13.2
378	507	racing	14.0	track	10.1
379	445	driving	14.0	cars	8.8
380	11	crouching	14.0	kneeling	28.1
381	74	autographing	13.9	blond	26.1
382	901	singing	13.9	girl	13.1
383	313	leaping	13.9	toys	21.6
384	346	packing	13.8	conveyor	18.2
385	508	paddling	13.8	person	15.3
386	267	saluting	13.8	soldiers	12.8
387	452	drumming	13.8	stage	18.0
388	944	massaging	13.8	back	6.0
389	595	juggling	13.8	throws	6.3
390	224	paddling	13.8	day	4.3
391	619	shredding	13.8	machinery	7.0
392	512	juggling	13.7	t-shirt	7.2
393	160	autographing	13.7	paper	11.7
394	390	pouring	13.7	liquid	21.1
395	394	paddling	13.7	car	5.3
396	541	flossing	13.6	fancy	8.9
397	396	massaging	13.6	electronical	6.6
398	321	standing	13.4	performing	9.8
399	432	weeding	13.4	garden	16.3
400	71	bulldozing	13.3	tractor	13.7
401	596	drenching	13.3	window	30.0
402	177	autographing	13.3	broadcast	2.3
403	10	dialing	13.3	jack	13.6
404	527	autographing	13.3	street	5.2
405	837	drenching	13.3	rain	9.6
406	293	leaping	13.3	fly	5.8
407	867	dropping	13.3	bunch	3.7
408	426	weeding	13.3	gardening	11.1
409	280	leaping	13.3	dog	20.5
410	331	autographing	13.1	contract	4.4
411	523	leaping	13.1	dancing	8.8
412	741	singing	13.0	microphone	12.5
413	744	barbecuing	13.0	chef	19.5
414	724	sawing	13.0	tree	5.6
415	277	juggling	13.0	motion	3.9
416	16	dialing	12.9	device	4.9
417	984	destroying	12.9	tower	11.4
418	917	dragging	12.9	pulling	20.1
419	729	leaping	12.8	running	7.2
420	365	autographing	12.8	walk	7.5
421	282	dropping	12.7	backdrop	8.9
422	443	frying	12.7	food	15.1
423	676	rinsing	12.7	bath	28.6
424	578	grilling	12.6	meat	3.8
425	994	autographing	12.5	bitter	7.7
426	391	locking	12.5	staircase	8.0
427	155	massaging	12.5	brown	18.1
428	920	competing	12.5	player	14.6
429	204	autographing	12.5	conference	3.4
430	959	manicuring	12.5	purplish	13.8
431	896	bandaging	12.5	tape	4.8
432	820	peeling	12.4	cutting	5.6
433	835	drumming	12.4	circle	12.5
434	202	dropping	12.4	surface	3.7
435	983	rinsing	12.3	scrubbing	5.6
436	519	autographing	12.3	camera	7.4
437	945	lecturing	12.3	talking	6.2
438	754	paddling	12.3	man	8.6
439	601	dropping	12.2	coffee	17.9
440	140	lecturing	12.2	suit	12.1
441	87	fueling	12.2	pickup	8.3
442	408	paddling	12.2	blue	7.0
443	333	draining	12.2	coming	17.4
444	979	lecturing	12.1	podium	8.4
445	871	falling	12.1	waterfall	10.7
446	53	paddling	12.1	seen	7.5
447	32	paddling	12.1	jeans	1.7
448	488	pedaling	12.1	bike	5.3
449	839	pushing	12.1	pushing	20.8
450	378	dunking	12.1	court	3.7
451	489	applauding	12.1	crowd	4.0
452	999	leaping	12.1	children	4.6
453	339	skating	12.1	skateboarding	22.0
454	653	dropping	12.1	slow	6.0
455	225	autographing	12.1	city	6.3
456	30	leaping	12.0	dog	19.8
457	654	applauding	12.0	old	12.1
458	102	tattooing	12.0	drawing	10.9
459	662	autographing	12.0	older	14.0
460	219	talking	12.0	turned	5.5
461	99	dropping	12.0	cartoon	13.3
462	669	shaving	11.9	legs	11.4
463	962	dropping	11.9	winds	7.4
464	205	sleeping	11.9	child	10.5
465	936	dropping	11.9	image	15.2
466	728	applauding	11.9	rally	12.5
467	804	leaping	11.9	field	12.0
468	529	leaping	11.9	dog	4.9
469	971	hitchhiking	11.8	road	19.4
470	666	applauding	11.8	smiling	13.7
471	797	applauding	11.7	black-n-white	11.6
472	425	drumming	11.7	filming	3.1
473	663	peeling	11.6	waist	5.3
474	471	applauding	11.6	hands	10.8
475	711	leaping	11.5	children	7.8
476	611	sleeping	11.5	dog	8.1
477	715	paddling	11.5	blue	7.8
478	36	singing	11.5	microphone	24.7
479	700	tattooing	11.4	someone's	3.2
480	1017	applauding	11.4	standing	6.1

Table 6: continued

Rank	Code	Visual Action Top Hypothesis label	Prc.	Spoken word Top Hypothesis word	F1	Rank	Code	Visual Action Top Hypothesis label	Prc.	Spoken word Top Hypothesis word	F1
481	887	autographing	11.4	sidewalk	4.7	541	982	mopping	9.8	floor	16.7
482	829	leaping	11.4	cat	14.5	542	115	autographing	9.7	yelling	7.6
483	162	lecturing	11.4	speaking	7.3	543	179	sleeping	9.7	tiger	13.2
484	852	swimming	11.3	pool	15.4	544	877	autographing	9.7	at	1.6
485	353	paddling	11.2	trickling	2.1	545	84	paddling	9.7	going	7.8
486	998	paddling	11.2	green	22.4	546	132	autographing	9.7	people	2.7
487	565	manicuring	11.2	painting	8.6	547	902	autographing	9.7	another	2.6
488	129	drumming	11.2	night	25.9	548	383	paddling	9.6	buildings	4.8
489	21	paddling	11.2	going	7.6	549	124	drumming	9.6	silhouette	3.7
490	690	autographing	11.2	blond	7.2	550	986	paddling	9.6	sliding	14.0
491	214	slipping	11.1	snow	11.0	551	253	applauding	9.5	tennis	5.7
492	454	paddling	11.1	bridge	5.6	552	761	autographing	9.5	ground	5.4
493	320	unpacking	11.1	boxes	18.2	553	925	rafting	9.5	group	13.9
494	261	paddling	11.1	down	3.4	554	90	drumming	9.4	wearing	10.2
495	864	sleeping	11.1	father	7.1	555	583	autographing	9.4	standing	7.9
496	411	burying	11.0	hole	16.0	556	725	hammering	9.4	blacksmith	11.1
497	127	competing	11.0	field	5.2	557	976	peeling	9.4	closing	12.9
498	580	child+singing	10.8	girl	10.7	558	922	drenching	9.4	driving	16.8
499	849	paddling	10.8	slowly	8.4	559	198	singing	9.4	tide	9.1
500	285	autographing	10.7	dress	8.1	560	144	screwing	9.4	machine	7.3
501	721	autographing	10.7	middle-aged	2.6	561	607	extinguishing	9.4	spraying	22.7
502	88	leaping	10.7	wall	10.1	562	195	racing	9.4	cars	23.0
503	769	autographing	10.6	table	10.2	563	913	drumming	9.3	sitting	6.6
504	91	autographing	10.6	she	8.1	564	366	bulldozing	9.3	trainer	2.6
505	119	jumping	10.6	rope	8.8	565	703	leaping	9.3	cats	4.3
506	448	paddling	10.6	hat	8.3	566	367	autographing	9.3	holding	6.8
507	831	skating	10.5	park	20.6	567	377	autographing	9.3	hallway	11.8
508	906	leaping	10.5	store	9.6	568	173	raining	9.2	cartoon	25.4
509	344	discussing	10.5	restaurant	25.7	569	86	competing	9.2	field	13.1
510	847	cheering	10.5	competition	4.3	570	328	autographing	9.2	walking	13.2
511	357	shaving	10.4	his	5.3	571	258	leaping	9.2	kids	7.1
512	904	running	10.4	running	13.1	572	487	autographing	9.2	giving	1.5
513	193	paddling	10.4	someone	16.2	573	385	ironing	9.2	clothes	15.8
514	192	applauding	10.3	motocross	6.2	574	598	raining	9.1	cartoon	17.6
515	230	autographing	10.3	looking	10.8	575	128	surfing	9.1	standstill	9.8
516	534	sleeping	10.3	bag	4.5	576	851	lecturing	9.1	upside	12.5
517	550	peeling	10.2	bowl	15.7	577	649	pouring	9.1	concrete	11.1
518	159	autographing	10.2	ward	4.3	578	695	sleeping	9.1	couch	12.8
519	314	leaping	10.2	mixed-race	4.0	579	70	autographing	9.1	people	4.4
520	709	leaping	10.1	animals	4.8	580	197	yawning	9.1	couch	30.6
521	95	sprinkling	10.1	sprinkler	10.8	581	446	applauding	9.0	many	8.8
522	227	sleeping	10.1	oh	2.7	582	351	singing	9.0	bright	3.2
523	935	applauding	10.1	perch	12.5	583	287	paddling	9.0	bird	15.2
524	176	typing	10.1	office	5.3	584	821	drumming	9.0	kayakers	3.8
525	1011	drumming	10.0	boy	17.0	585	310	applauding	9.0	smiling	12.9
526	683	competing	10.0	game	7.1	586	203	paddling	8.9	video	3.7
527	185	knitting	10.0	stitching	8.2	587	624	crushing	8.9	greenfield	20.3
528	289	dropping	10.0	ground	16.5	588	696	autographing	8.9	man	9.7
529	899	reaching	10.0	church	20.8	589	514	paddling	8.9	behind	2.8
530	767	playing	10.0	overwatch	6.7	590	886	falling	8.9	shine	5.6
531	796	paddling	10.0	base	3.7	591	451	peeling	8.9	carrots	5.2
532	161	discussing	9.9	family	10.8	592	953	autographing	8.8	outside	12.5
533	782	leaping	9.9	doing	12.9	593	975	paddling	8.8	building	1.8
534	850	autographing	9.9	american	1.9	594	643	carving	8.8	working	12.4
535	620	leaping	9.8	bridge	4.1	595	418	autographing	8.8	suit	13.1
536	992	leaping	9.8	point-of-view	6.9	596	481	autographing	8.7	woman	9.1
537	547	grilling	9.8	crawling	17.3	597	756	paddling	8.7	wearing	3.2
538	891	paddling	9.8	on	2.5	598	670	signing	8.7	table	7.2
539	340	dusting	9.8	clean.	5.2	599	785	autographing	8.7	standing	2.1
540	659	storming	9.8	yard	18.2	600	787	drumming	8.7	sitting	7.5

Table 6: continued

Rank	Code	Visual Action Top Hypothesis label	Prc.	Spoken word Top Hypothesis word	F1	Rank	Code	Visual Action Top Hypothesis label	Prc.	Spoken word Top Hypothesis word	F1
601	723	autographing	8.7	something	6.1	661	980	kicking	7.7	shooting	12.5
602	719	talking	8.7	toddler	17.9	662	238	sleeping	7.7	squirrel	12.8
603	209	autographing	8.7	hair	8.4	663	360	injecting	7.7	person	2.9
604	521	rafting	8.7	people	8.4	664	853	camping	7.7	tent	8.9
605	98	applauding	8.6	stand	6.2	665	652	autographing	7.6	single	1.5
606	969	leaping	8.6	kids	7.2	666	893	watering	7.6	watering	8.4
607	770	flossing	8.6	explaining	7.5	667	546	piloting	7.6	lyrics	3.4
608	616	leaping	8.5	snow	20.0	668	674	applauding	7.6	night	8.4
609	410	erupting	8.5	explodes	7.5	669	881	autographing	7.5	table	7.6
610	12	paddling	8.5	distance	13.6	670	236	hammering	7.5	wooden	9.5
611	750	flossing	8.5	drinking	8.5	671	778	leaping	7.5	house	8.7
612	1009	autographing	8.5	street	17.1	672	260	flossing	7.5	smiling	19.2
613	463	slicing	8.5	pieces	11.7	673	399	paddling	7.5	of	6.5
614	843	autographing	8.5	speaking	4.8	674	146	autographing	7.5	language	4.9
615	772	paddling	8.5	workers	12.7	675	745	autographing	7.5	sitting	10.0
616	781	leaping	8.5	involving	7.4	676	207	paddling	7.5	man	12.5
617	757	flossing	8.4	caption	10.4	677	732	smelling	7.5	flowers	36.6
618	793	pointing	8.3	gameplay	16.7	678	647	autographing	7.4	smashes	3.3
619	403	racing	8.3	car	5.3	679	894	splashing	7.4	plastic	9.2
620	988	clipping	8.3	shoe	8.3	680	416	drumming	7.4	group	9.8
621	502	paddling	8.3	going	1.5	681	492	autographing	7.4	fans	1.4
622	343	paddling	8.3	over	2.7	682	467	drumming	7.4	child	8.0
623	450	shaving	8.3	chef	5.2	683	573	wrapping	7.4	box	9.8
624	765	paddling	8.2	gymnast	4.8	684	381	autographing	7.4	he	3.0
625	476	paddling	8.2	trees	8.4	685	855	autographing	7.3	gentleman	2.6
626	818	autographing	8.2	vest	3.3	686	939	peeling	7.3	close	7.0
627	746	autographing	8.2	street	13.7	687	494	peeling	7.3	hands	4.9
628	122	applauding	8.2	people	7.8	688	575	paddling	7.3	a	6.0
629	275	leaping	8.2	workout	4.2	689	581	smashing	7.3	building	21.9
630	592	hammering	8.2	piles	3.9	690	142	stopping	7.3	characters	11.4
631	1003	leaping	8.2	around	5.9	691	599	autographing	7.3	two	5.6
632	7	paddling	8.1	and	3.2	692	309	paddling	7.2	shooting	4.8
633	257	raining	8.1	blown	20.7	693	264	drumming	7.2	bedroom	3.6
634	170	leaping	8.1	running	5.5	694	919	autographing	7.2	hands	12.4
635	341	flossing	8.1	how	6.1	695	47	autographing	7.2	woman	6.4
636	354	sewing	8.1	machine	14.2	696	570	paddling	7.1	we	2.0
637	600	paddling	8.1	each	6.1	697	965	paddling	7.1	red	3.4
638	677	rolling	8.1	cooks	6.9	698	361	autographing	7.1	upright	3.6
639	133	sleeping	8.1	string	7.3	699	934	peeling	7.1	putting	7.9
640	678	leaping	8.0	tree	7.5	700	594	sitting	7.1	inject	8.0
641	466	injecting	8.0	close	18.2	701	186	draining	7.1	house	20.9
642	1006	stirring	8.0	pot	5.2	702	809	paddling	7.1	man	11.0
643	212	crying	8.0	helping	7.0	703	783	paddling	7.1	with	1.6
644	889	autographing	8.0	young	4.0	704	151	autographing	7.0	store	6.5
645	437	manicuring	7.9	fingers	8.3	705	474	paddling	7.0	person	9.2
646	468	jumping	7.9	motorcycle	9.9	706	1021	paddling	7.0	decorated	8.9
647	633	applauding	7.9	show	7.9	707	359	paddling	7.0	picture	5.7
648	59	drumming	7.9	watching	14.2	708	740	applauding	6.9	people	6.1
649	814	peeling	7.9	someone	4.7	709	614	autographing	6.9	knick-knack	5.3
650	441	leaping	7.9	jeans	14.1	710	237	leaping	6.9	inflating	6.7
651	775	inflating	7.9	chair	16.5	711	567	autographing	6.9	and	2.8
652	46	autographing	7.9	woman	23.8	712	135	signing	6.9	sitting	6.6
653	824	autographing	7.9	field	2.3	713	506	drumming	6.9	guys	7.3
654	968	dusting	7.9	floor	5.4	714	28	autographing	6.9	hey	7.0
655	544	reaching	7.8	climbing	13.0	715	456	applauding	6.9	animated	4.9
656	389	autographing	7.8	front	14.3	716	768	autographing	6.9	holding	7.4
657	819	lecturing	7.8	laughing	18.1	717	879	leaping	6.9	exercising	5.1
658	498	shaving	7.8	pink	18.5	718	628	drumming	6.9	men	10.4
659	9	paddling	7.7	green	5.2	719	80	discussing	6.9	women	8.6
660	927	singing	7.7	saying	13.9	720	586	applauding	6.8	haired	7.7

Table 6: continued

Rank	Code	Visual Action Top Hypothesis		Spoken word Top Hypothesis		Rank	Code	Visual Action Top Hypothesis		Spoken word Top Hypothesis	
		label	Prc.	word	F1			label	Prc.	word	F1
721	1004	pouring	6.8	color	6.8	734	167	peeling	6.7	into	3.5
722	72	injecting	6.8	mixing	4.7	735	428	leaping	6.7	doing	2.2
723	876	autographing	6.8	arena	3.8	736	300	paddling	6.6	is	2.3
724	878	gambling	6.8	game	9.4	737	786	paddling	6.6	background	1.7
725	114	paddling	6.8	man	15.7	738	272	leaping	6.6	truck	8.5
726	764	raising	6.8	trash	10.0	739	297	applauding	6.6	rustic	4.5
727	326	leaping	6.8	zooming	3.1	740	303	paddling	6.6	down	1.0
728	217	surfing	6.8	surfer	2.0	741	93	paddling	6.5	car	3.3
729	107	pouring	6.8	bottle	5.8	742	542	baking	6.5	cupcake	9.2
730	749	injecting	6.7	person's	2.2	743	733	discussing	6.5	men	7.3
731	612	autographing	6.7	disgust	4.8	744	23	leaping	6.5	cross	5.5
732	834	autographing	6.7	outside	12.7	745	104	injecting	6.5	beard	2.6
733	655	marrying	6.7	couple	7.5	746	279	leaping	6.5	garden	4.4